*International Journal of Engineering Research and Development*
*e- ISSN: 2278-067X, p-ISSN: 2278-800X, www.ijerd.com*
*Volume 21, Issue 12 (December 2025), PP 14-32*

# Integrated Petrophysical, Seismic, and Volumetric Evaluation of the QX Field, South-eastern Niger Delta, Nigeria

*Ekiliwo Nnenna Justina[1], Anietie E Ekot[2], Itoro G. Udo[3]
[1,2,3]*Akwa ibom state university, Nigeria*

***Abstract***
*This study presents a comprehensive petrophysical and depositional environment evaluation of the QX Field, located in the Southeastern Niger Delta. The aim was to integrate well log analysis, and seismic attribute evaluation to characterize the reservoir properties and estimate hydrocarbon potential. Three key reservoirs (RES 1, RES 2, and RES 3) were delineated using gamma ray, resistivity, density, and neutron logs, followed by quantitative petrophysical analysis. Net-to-gross (NTG) values ranged from 69.25% to 84.75%, with effecti ve porosity between 19.5% and 23.25%, shale volume ranging from 12.20% to 30.75%, and water saturation from 57.75% to 94.75%. Permeability varied across reservoirs from 59.68 mD to 152.51 mD, indicating fair to good reservoir quality. Volumetric estimation using mapped areas and log-derived parameters yielded Stock Tank Oil Initially in Place (STOIIP) values of 6.13 MMSTB (P50) for RES 1 and 58.27 MMSTB (P50) for RES 3. RES 2 was identified as a gas-bearing interval with 9.54 BCF (P50) GIIP. The total most likely (P50) volumes for the QX Field are 64.40 MMSTB of oil and 12.20 BCF of gas.*
***Keywords:*** *Petrophysical, Reservoir, Lithology, Wells and depositional environment.*

---

Date of Submission: 01-12-2025 Date of acceptance: 10-12-2025

---

## I. Introduction

The Niger Delta Basin is an economically significant and complex geological region extending from Nigeria to the Gulf of Guinea. It develops because of swift deposition of sediments without effective sediment dewatering (IheaturThe exploration and exploitation of hydrocarbon resources demand a thorough understanding of the geological settings in which reservoir rocks were deposited. The Niger Delta Basin, one of the world's most prolific petroleum provinces, offers an ideal setting for such investigations due to its complex stratigraphy, diverse depositional environments, and well-established hydrocarbon systems. The basin, which has developed since the Late Cretaceous in response to the rifting and separation of the South American and African plates, is located on the passive continental margin of West Africa. It extends over 75,000 km² and encompasses thick sequences of sediments deposited in a variety of continental to marine environments. (Evamy et al.,1978).

The Niger Delta is stratigraphically composed of three main formations that reflect a regressive deltaic sequence: the Akata Formation at the base, made up of over-pressured marine shales and minor turbiditic sandstones, serving as the primary source rock; the Agbada Formation in the middle, which contains alternating sandstones and shales deposited in delta front to delta plain environments, forming the main hydrocarbon reservoirs and seals; and the uppermost Benin Formation, consisting of fluvial and alluvial continental sands that represent the exposed surface of the modern delta. (Short and Stauble,1967).

The QX Field, situated in the Southeastern Niger Delta, lies within a tectonically stable region influenced by listric faulting and growth structures common to the delta. This area showcases a dynamic interplay of fluvial, tidal, and shallow marine processes, which control the nature and distribution of sedimentary facies. In such settings, the environment of deposition (EOD) plays a fundamental role in determining the spatial distribution, geometry, and petrophysical quality of reservoir sands factors that are critical to hydrocarbon prospectivity and production (Weber & Daukoru, 1975).

The EOD directly influences key reservoir quality attributes such as porosity, permeability, grain size distribution, and internal heterogeneity. These parameters, in turn, govern fluid storage and movement within the subsurface (Selley, 1978; Allen, 1965). Deltaic distributary channels, tidal flats, shoreface complexes, estuarine fills, and marine turbidites all of which are characteristic of the Niger Delta exhibit distinct sedimentological signatures and reservoir geometries (Weber & Daukoru, 1975; Doust & Omatsola, 1990). Therefore, an accurate understanding of these depositional systems in the QX Field is essential to predicting reservoir continuity, connectivity, and performance.

A qualitative and quantitative evaluation of the QX Field requires an integrative methodology that combines multiple geological and geophysical datasets. Well log analysis, core interpretation, sedimentological

facies classification, and seismic attribute analysis are key to decoding the depositional environments and their influence on reservoir distribution and quality (Rider & Kennedy, 2011). These tools support the reconstruction of paleoenvironments and facies architecture, enabling the identification of sand-prone zones, estimation of net-to-gross ratios, and prediction of the lateral extent of reservoirs.

Moreover, the hydrocarbon potential of any field is inherently tied to its geological history and stratigraphic evolution. In the QX Field, deciphering the depositional framework enables the identification of reservoir sweet spots, the assessment of compartmentalization risks, and the estimation of hydrocarbon-in-place volumes. A clear grasp of these geological factors is critical for improved reservoir modelling, reduced exploration risk, and optimized field development strategies.

This research is therefore designed to carry out a comprehensive depositional and petrophysical evaluation of the QX Field. By integrating qualitative sedimentological interpretations with quantitative petrophysical and seismic data, the study aims to unravel the depositional history and assess the hydrocarbon potential of the field. The findings are expected to enhance the understanding of sedimentary processes in the Southeastern Niger Delta and contribute to more accurate predictive models for reservoir quality and distribution.

The Niger Delta is known worldwide as one of the richest hydrocarbon basins, yet some areas, like the Q-X field in the southeastern part, are still not fully explored, hence the field history not understood.

Even though the Niger Delta plays a huge role in Nigeria's oil and gas production, there are still major hurdles when it comes to accurately identifying hydrocarbon-rich zones, elucidating the complexities of the reservoirs and assessing fluid saturation. While there's been a lot of research on the depositional environments of the Niger Delta, especially in the Agbada Formation where most hydrocarbon reservoirs are found, the Q-X Field is lacking detailed petrophysical and sedimentological studies. This gap leads to significant uncertainties regarding the quality of the reservoirs, how fluids are distributed, and the overall hydrocarbon potential.

One of the main problems encountered is lack of thorough reservoir characterization in the Q-X Field. Without comprehensive petrophysical assessments, it might be difficult to unravel the unknown reservoir characteristics such as porosity, permeability, and fluid saturation. When we don't have accurate data on these properties, it becomes tough to evaluate the true potential of the reservoirs, which can result in less effective exploration and production strategies.

## II. Location Of The Study Area

The study area Q-X field is in the southeastern region of the Niger Delta basin. It lies within the onshore transition zone of the delta, which is marked by a complex interaction of fluvio-deltaic, delta-front, and pro-deltaic environments. The Niger Delta area is generally found between approximately Latitude 3°N and 6°N, and Longitude 4°E and 8°E, it's location in the southeastern Niger Delta situates it within a zone that has undergone gravitational tectonics, substantial sediment accumulation, and the formation of various structures, including listric normal faults and shale-related features (Fig. 1)

The Q-X Field serves as a key case study in this research, showing an ideal example of how the Niger Delta's major tectonic phases control depositional sequences, structural deformation, and hydrocarbon trapping mechanisms.features (Fig. 2)

Fig.1: Map of Nigeria, showing the study area. (Bolaji,2024).

## III. Geology Of The Niger Delta

The Niger Delta, one of the world's largest and most prolific deltaic systems, is situated at the apex of the Gulf of Guinea on the West African continental margin. Its immense hydrocarbon reserves and complex geological architecture are fundamentally products of a unique and protracted tectonic evolution intricately linked to the breakup of the supercontinent Gondwana and the opening of the South Atlantic Ocean (Burke,1969). Understanding this tectonic framework is paramount to comprehending the basin's formation, structural styles, sediment infill, and ultimately, its vast petroleum potential. The genesis of the Niger Delta Basin is rooted in the extensional tectonics that commenced in the Late Jurassic, marking the initial stages of the separation of the African and South American continents. This continental rifting established a series of rift basins that would later evolve into the passive continental margins of the South Atlantic. (Whiteman,1982).

The rifting process was characterized by the development of a Y-shaped or "rift-rift-rift" triple junction. Two arms of this triple junction successfully opened to form the South Atlantic Ocean (proto-Atlantic), leading to seafloor spreading and the eventual separation of the continents. The third arm, which failed to develop into a full oceanic basin, extended inland as the Benue trough (Burke et al.,1971). The Benue Trough is a prominent, NE-SW trending rift basin stretching over 1000 km into the African craton. It represents the "failed arm" or "aulacogen" of the triple junction. During the Early Cretaceous (Aptian to Albian), the Benue Trough experienced significant subsidence and received a thick succession of marine and paralic sediments (Cratchley and Jones,1965). While not directly part of the active Niger Delta depositional system, its tectonic history significantly influenced the regional stress regime and sediment provenance for the developing delta. Early movements along major NE-SW trending faults within this failed rift system led to the formation of the Abakaliki Trough, a depocenter for Cretaceous sediments (Murat,1990). This initial rift phase involved significant crustal stretching and thinning, leading to heat flow and localized volcanism (Doust & Omatsola, 1990). The pre-rift basement, composed primarily of Precambrian metamorphic and igneous rocks of the West African Craton, was fractured and downfaulted, creating the foundational architecture for subsequent sedimentation (Kulke,1995).

Following the initial rifting and the onset of seafloor spreading, the tectonic regime transitioned from active extension to passive margin subsidence. This stage was primarily driven by thermal subsidence and load-induced subsidence. As the lithosphere cooled and contracted after the rifting phase, it underwent thermal subsidence, causing a regional down warping of the continental margin (Allen & Allen,2005). This created accommodation space for the immense volumes of clastic sediments that would later form the Niger Delta. The sheer weight of the accumulating sediments (sedimentary load) further contributed to subsidence, creating a feedback loop where deposition led to more subsidence, which in turn allowed for more deposition. (Kulke,1995).

Growth faults, while acting as seals in many cases, can also serve as conduits for hydrocarbon migration from deeper source rocks into shallower Agbada Formation reservoirs. Fault-related fracturing and pressure differences facilitate this movement (Ejedawe,1981). The pervasive gravity tectonics generated abundant structural traps (rollover anticlines, fault closures, mud diapir-related traps) and stratigraphic traps (e.g., pinch-outs against growth faults) within the Agbada Formation. The interbedded shales within the Agbada serve as excellent seals, (Weber & Daukoru,1975). The continuous nature of the delta's progradation means that hydrocarbon generation, migration, and trap formation are ongoing processes. As the delta progrades, older source rocks are buried deeper and mature, while new traps are continuously being formed and charged. This dynamic "fill-and-spill" model contributes to the basin's sustained productivity (Stacher,1995).

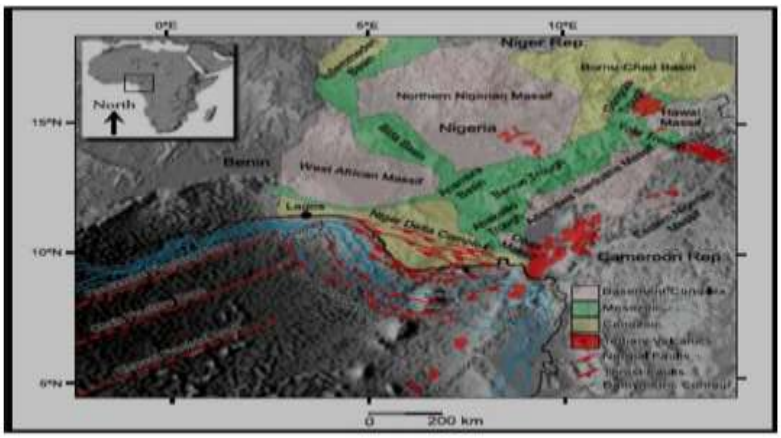


Fig.2: Location Map of the Niger Delta Region Showing the Main Sedimentary Basins and Tectonic feature (Olowokere et al., 2019)

## IV. Materials And Methods

Data sets from "Q-X" Marginal field reservoirs were obtained from an oil producing company in the Niger Delta with the cooperation of the Nigerian Upstream Petroleum Regulatory Commission (NUPRC). These data sets contained the following:

- Digitized wireline log in LAS.
- Check shots.
- Well deviation data.
- Seismic data.

The data was analyzed and interpreted using the following software: Schlumberger Petrel, interactive petrophysics, and Microsoft Excel.

Table 1: Well Inventory


Table.2: Vintage seismic properties of Q-X Field

| | 3D SEISMIC DATA |
|---|---|
| Format | SEGY – Post Stack |
| Total Coverage Area | 54.78 $km^2$ |
| Inline Range | 5800 – 6200 |
| Cross line Range | 1480 – 1700 |
| Sample Interval | 4 |
| Time Range | 0 – 6000 |

**RESEARCH DESIGN (WORKFLOW)**

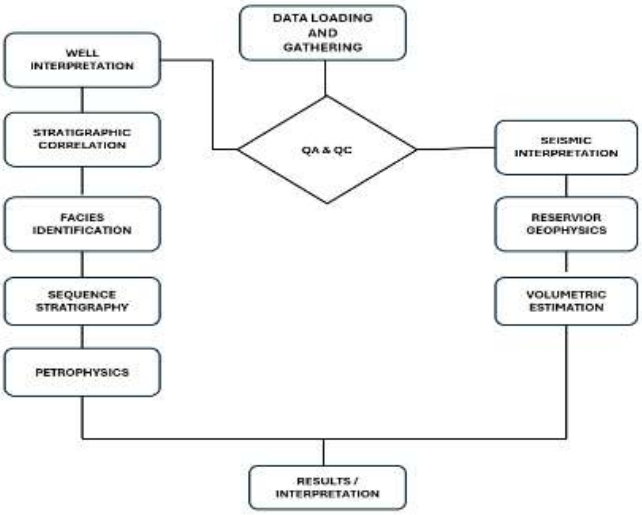


Figure 3.: shows the workflow that guided the result/ interpretation of the study.

## V. Methodology

**Data Loading**

The data loading process into Petrel involves several steps to ensure accurate importations into the software environment. Importing well heads and logs is the first step in the data loading procedure. The well head file carries the well's name, surface position (2D-XY coordinate system), Kelly bushing (Kb), top depth, and bottom depth. This permits well placements to be displayed on the base map. Each well's check shot, deviation, and log data were then imported. The seismic volume was imported using SEG-Y format.

**Well Normalization**

Well normalization involved adjusting well log data to a common scale or reference system to ensure consistency and comparability across multiple wells in a reservoir. It is a critical step in subsurface modeling and reservoir characterization, as it helps to remove any inconsistencies caused by varying logging conditions, operational differences, or measurement units. To normalize the wells, the log tracts were scaled from 1-150 API for the gamma ray log, 0.2-2000-ohm meters for the resistivity log, 1.65-2.65g/cm3 for the density log, 0-0.6 for the neutron porosity log, and 40-140 for the sonic log. Each log track was assigned to a distinct color.

**Reservoir Identification / Well Correlation**

This process begins by identifying and correlating formation tops to develop a chronostratigraphic framework for the field. The wells were all arranged along strike lines West to East which correspond with their location and relative distance to each as observed on the base map. Correlation of the wells was carried out to develop a lateral continuity for each identified horizon (sand interval) across the three wells in the field with the use of the only lithology log available (GR-log) alongside with the resistivity logs to check the fluid contents present within the sediments i.e. hydrocarbon or water.

**Petrophysical Analysis**

Petrophysical analysis involves analyzing log data to calculate key reservoir properties such as porosity, permeability, water saturation, and hydrocarbon saturation. These properties are essential for characterizing the reservoir's ability to store and transmit fluids. Sand thicknesses was estimated with a view to determine areas with good sand development, other petrophysical analysis carried out included estimation of sand/shale percentages, estimation of porosity, estimation of water and hydrocarbon saturation, delineation of possible hydrocarbon-bearing sands and also water, oil and gas contacts, estimation and comparison of porosity, permeability, water saturation, hydrocarbon saturation in and across the well(s) using the available wireline logs, estimation of shale volume content, bulk volume water, hydrocarbon pore volume/thicknesses, Net pay flag, cross plots of variable parameters, such as the different porosity logs.

**Net-to-Gross Ratio (NTG)**

Net thickness is often used alongside gross thickness to calculate the net-to-gross ratio (NTG), which represents the proportion of the gross interval that is productive. The Net-to-gross ratio was determined using the formula below:

NTG=(Net Thickness)/(Gross Thickness) (1)

**Porosity**

Porosity is the proportion of a given volume of rock that forms pore space and can thus hold liquid (Schlumberger, 1985). It is the fractional volume of pores in a rock, a relative quantity that is often expressed in decimal/fractional units or as a percentage. This volume of voids is useful for storing fluids like water, oil, and gas; if permeable, it may also transport these fluids to a lower-pressure zone. The porosity was estimated by inputting the bulk density measurements acquired from the density log within each reservoir into the following equation:

$$\emptyset_{\mathbf{T}} = \frac{\rho_{\mathbf{mat}} - \rho_{\mathbf{bulk}}}{\rho_{\mathbf{mat}} - \rho_{\mathbf{fluid}}} \quad (2)$$

Where:

ρ_mat = Density of sandstone

ρ_bulk = Bulk Density

ρ_fluid = Fluid Density

where density for sandstone is=2.65g/ cm3

fluid density=1

**Estimate of Shale Volume**

Shale volume (Vsh) is a critical parameter in reservoir characterization as it helps distinguish between clean reservoir rocks and shaly intervals. It is essential for determining the net pay, effective porosity, and overall reservoir quality. Shale volume was estimated using the gamma-ray (GR) log.

Gamma Ray Index (IGR) is shown as:

$$\mathbf{I_{GR}} = \frac{\mathbf{GR_{log}} - \mathbf{GR_{min}}}{\mathbf{GR_{max}} - \mathbf{GR_{min}}}$$

where: IGR = Gamma ray index
GRlog = Gamma ray reading of the Formation,
GRmin = Minimum gamma ray (clean sand),
GRmax = Maximum gamma ray (shale).
Using Larionov (1969) equation for tertiary rocks:

$$Vsh = 0.0083(2^{3.7 \times IGR} - 1) \quad (4)$$

**Water Saturation**

Water saturation (Sw) is a crucial petrophysical parameter in reservoir characterization, representing the fraction of pore space in a rock that is occupied by formation water. It is critical for determining hydrocarbon saturation (Sh), volumetric reserves, and production potential. Accurate estimation of Sw is essential for evaluating reservoir quality and planning hydrocarbon extraction.

Water saturation is expressed as a percentage or fraction:
Sw=

$$S_w = \frac{\text{Volume of Water in Pores}}{\text{Total Pore Volume}}$$

For this study, Water saturation was calculated using the Archie's Equation below

Where: $\mathbf{S_w^n} = \frac{\mathbf{a}}{\mathbf{\emptyset^m}} . \frac{\mathbf{R_w}}{\mathbf{R_t}}$ (5)

Sw = Water saturation
Rw = Formation water resistivity
Rt = True formation resistivity
Φ = Porosity
A = Tortuosity factor (1)
m = Cementation exponent (typically 1.8–2.0 for sandstones)
n = Saturation exponent (typically 2.0 for water-wet rocks)

Seismic Interpretation

Seismic interpretation is a critical component of subsurface exploration and reservoir characterization, involving the analysis of seismic data to understand geological structures, stratigraphy, and rock properties in the subsurface. In contrast to the one-dimensional nature of a well bore, seismic data allows for a good portrayal of the earth's extremely complicated three-dimensional subsurface.

Synthetic Seismogram Generation

The sonic log, which is the reciprocal of velocity, was calibrated using check shot data. The calibration process is necessary to improve the quality of the sonic log because the sonic log is prone to washouts and other wellbore related issues. The results of calibrating the sonic log with the check shot gives the calibrated sonic log.

The calibrated sonic log is used along with the density log to generate an acoustic impedance (AI) log. The acoustic impedance log is calculated for each layer of rock. The next step involves generating the reflectivity coefficient (RC) log. RC is calculated and generated using the AI log. The RC log generated is then convolved with a wavelet to generate a synthetic seismogram which is comparable with the seismic data. The statistical wavelet utilized for convolution is extracted from seismic data. The synthetic seismogram was generated. The mathematical expressions that govern the entire well-to-seismic tie workflow are presented below:

$$\mathbf{AI} = \boldsymbol{\rho}\mathbf{v}$$

$$\mathbf{RC} = \frac{\boldsymbol{\rho_2 v_2 - \rho_1 v_1}}{\boldsymbol{\rho_2 v_2 + \rho_1 v_1}} \quad (6)$$

Synthetic Seismogram = $\frac{\rho_2 v_2 - \rho_1 v_1}{\rho_2 v_2 + \rho_1 v_1}$ * wavelet

Where:
AI = acoustic impedance
RC = reflection coefficient
ρ = density
v = velocity.

Seismic to Well Tie

A seismic-to-well tie is a crucial step in seismic interpretation that ensures the alignment of seismic data with subsurface geological features recorded in well logs. It establishes a robust relationship between time-based seismic data and depth-based well log data, enabling interpreters to correlate seismic reflectors with specific geological horizons. This process improves the accuracy of seismic interpretation and provides a direct link between seismic imaging and reservoir properties.

Fault Mapping

Faulted structures are important elements of the petroleum system as they play important roles in the trapping of hydrocarbon, making it imperative to ensure the use of correct and adequate techniques to map them. Faults in the seismic survey were identified based on criteria such as abrupt termination of reflection events; breaks in reflection events; abrupt lateral velocity changes; overlapping of reflection events; pattern change of reflection events across a fault; structural deformation in beds above the fault zone; anomalous dip near the fault zone. The major faults in the seismic survey were identified and mapped along dip lines.

To have a good resolution of the faults, a scroll increment of 10 lines was employed on both inlines and cross lines while picking the faults. Precautions were also made to ensure the consistency of the fault traces owing to the possibility that faults dying out can easily be mistaken for another in a field with a complex fault system. To ensure consistency, a variance attribute was generated to amplify the discontinuities and guide the continual fault picking on subsequent lines.

Mapping of Horizons

Prior to the proper establishment of the stratigraphic framework of the field, identified stratigraphic horizons were mapped at every 5 msec on both inline and crossline across the seismic volume. The seeded horizon was used as input to generate the time surface maps for the horizons of interest.

Generation of Maps

Structural maps were generated from the mapped horizons that were picked on both cross line and inline to evaluate the geometry of the hydrocarbon zones. The horizon maps were generated in time, and the velocity model was used to produce a depth map to aid in the data interpretation.

Reservoir Geophysics

Seismic attributes will be extracted and analyzed for reservoir characterization, these include RMS (Root Mean Square) Amplitude to highlight high-amplitude zones indicative of potential hydrocarbon presence or thick sands; attributes like phase and frequency for continuity and discontinuity analysis, coherence/similarity to delineate faults, channels, and stratigraphic boundaries; and spectral decomposition to identify tuned intervals related to reservoir thickness and stratigraphy Chopra and Marfurt, (2007). These attributes will enhance the visualization of reservoir geometry, delineate hydrocarbon accumulation zones, identify fluid contacts, and reveal internal reservoir heterogeneities.

Volume Estimation (Hydrocarbon in Place)

Volume estimation quantitatively estimates the Stock Tank Oil Initially in Place (STOIIP) or Gas Initially in Place (GIIP) for identifying hydrocarbon accumulations Dake, (1978).

This begins with a detailed petrophysical evaluation of well logs for the net reservoir intervals, calculating parameters such as shale volume (V-shale) derived from the Gamma Ray log, and porosity ($\phi$) Asquith and Krygowski (2004). Water saturation (Sw) will be determined using appropriate petrophysical models, such as Archie's equation Archie (1942), with input parameters like cementation exponent (m), saturation exponent (n), and tortuosity factor (a). The Net-to-Gross Ratio (N/G) will be calculated as the proportion of reservoir-quality rock (meeting defined porosity, shale, and water saturation cut-offs) within the gross reservoir interval. These petrophysical parameters will then be averaged for each reservoir zone from the available wells. The Gross Rock Volume (GRV) determination will involve utilizing the structurally interpreted depth maps of the top and base of the reservoir unit, combined with the fault derived from reservoir geophysics, to accurately calculate the (GRV) of the hydrocarbon accumulation within volume calculation module.

Therefore, the hydrocarbon pore volume (HCPV) was calculated using the following standard volumetric formula:

$$HCPV=A\times h\times N/G\times\phi\times(1-Sw) \quad (7)$$

Where,

A = The Areal Extent

H = Gross Thickness (Both from Seismic Interpretation and Mapping),

N/G= Net-To-Gross Ratio,

Φ = Average Effective Porosity,

Sw = Average Water Saturation (All from Petrophysical Evaluation).

For Oil, Stoiip Will Be Calculated As

$$STOIIP=HCPV/Bo \quad (8)$$

Where:

Bo = Oil Formation Volume Factor

For gas, GIIP will be calculated as

$$GIIP=HCPV\times Fg \quad (9)$$

Fg = Gas Expansion Factor

Bo and Fg will be obtained from regional analogues. Finally, Monte Carlo simulation, is recommended to assess the uncertainty in the volumetric estimates Downey, (2005). This involves defining statistical distributions for key input parameters (A, h, N/G, ϕ, Sw, Bo/Fg) to generate P10 (optimistic), P50 (most likely), and P90 (pessimistic) hydrocarbon volume estimates.

To determine the final Total Field Volume, the P10, P50 and P90 values from the individual reservoir simulations must be aggregated probabilistically. Therefore, the Total Field P10 and P90 were calculated using the Variance Addition Method (Root Sum of Squares or RSS), assuming the individual reservoirs are statistically independent. (SPE, 2018)

The aggregation steps are:

- Mean (P50): The P50 values are summed arithmetically. $P50Total = \sum P50i$ (10)
- Standard Deviation($\boldsymbol{\sigma}$): The standard deviation for each reservoir (Ri) is estimated from the P10-P90 range, and then the variances ($\boldsymbol{\sigma}^2$) are summed:

$$\sigma_{Total} = \sqrt{\sum_i \left(\frac{P10_i - P90_i}{2.56}\right)^2} \quad (11)$$

- Probabilistic range: the total P10 and P90 are calculated using the total mean and standard deviation:

$$P\ x\ Total = P50\ Total \pm 1.28 \times \boldsymbol{\sigma}\ Total \quad (12)$$

- This method correctly accounts for the portfolio effect, resulting in a statistically valid and narrower uncertainty range for the total field volume.

## VI. Results And Discussion

WELL LOG CORRELATION AND RESERVOIR DELINEATION

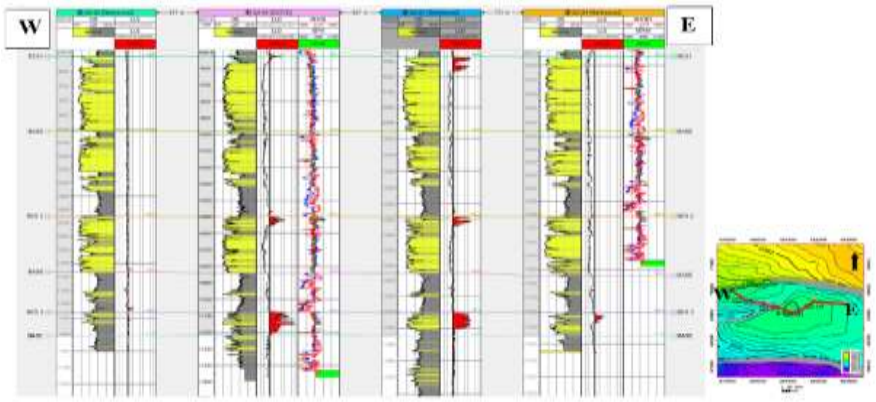


Figure 4.: Well log Correlation (sand cut-off: 60API)

A field wide correlation along strike from East to West using wells QX-02, QX-05, QX-01 and QX-04 was carried out by integrating gamma ray log, resistivity logs, density and Neutron porosity log. Tops and bases of three reservoirs (RES1, RES2 and RES3) were mapped using resistivity as a log-based hydrocarbon indicator (Figure 4). The occurrence and distribution of the lithostratigraphic units appear to reflect influence of basin morphology and sea level rise. There reservoirs are expressively continuous across all the wells in thickness and geometry. Sand thick fairly appears to decrease in some reservoirs in the east direction reflecting the character of deposition in the Niger Delta basin (Tuttle et al., 1999).

**PETROPHYSICAL EVALUATION**

Table 3 shows the summary of the reservoirs petrophysical evaluation, with emphasis on Net-to-Gross (NTG), effective porosity (PHIE), Volume of Shale (VSH), Water Saturation (Sw) and Permeability (K) in QX Field.

Generally, QX field reservoir Net-to-Gross values ranges from 60% to 87%, Effective porosity is between 18% to 25%, Volume of shale ranges from 13% to 40%, Water Saturation ranges from 20% to 99% and Permeability ranges from 37.28mD to 219.73mD. The reservoirs have fair to good qualitative results based on table 4.1 below. These values however are comparable to those reported in the Niger Delta. In addition, it was observed that reservoir properties decreased with depth and notably the thickness also.

Table 2: Combined porosity and permeability classification chart (Etu-Efeotor, 1997)

| **Reservoir quality** | **Porosity (%)** | **Permeability (mD)** |
|---|---|---|
| **Excellent** | >25 | >1000 |
| **Good** | 20 – 25 | 100 -1000 |
| **Fair** | 15 – 20 | 10 – 100 |
| **Poor** | 10 -15 | 1 – 10 |
| **Very poor** | <10 | <1 |

Table 3: Result of the Petrophysical Evaluation

| **WELLS** | **RESERVOIR** | **GROSS (ft)** | **NET (ft)** | **NTG (%)** | **PHIE (%)** | **VSH (%)** | **Sw (%)** | **K (mD)** |
|---|---|---|---|---|---|---|---|---|
| **QX-01** | **RES 1** | 479 | 402.36 | 84 | 23 | 16 | 88 | 140.07 |
| | **RES 2** | 378 | 291.06 | 77 | 24 | 23 | 83 | 176.26 |
| | **RES 3** | 105 | 77.7 | 74 | 20 | 26 | 29 | 65.85 |
| | | | | | | | | |
| **QX-02** | **RES 1** | 508.5 | 417.06 | 82 | 23 | 18 | 100 | 140.07 |
| | **RES 2** | 410 | 328 | 80 | 22 | 20 | 100 | 110.18 |
| | **RES 3** | 62 | 42.16 | 68 | 18 | 32 | 98 | 37.28 |
| | | | | | | | | |
| **QX-04** | **RES 1** | 507 | 441.09 | 87 | 22 | 13 | 98 | 110.18 |
| | **RES2** | 399 | 303.24 | 76 | 24 | 24 | 99 | 176.26 |
| | **RES3** | 121 | 72.6 | 60 | 19 | 40 | 82 | 49.92 |
| | | | | | | | | |
| **QX-05** | **RES 1** | 392 | 337.12 | 86 | 25 | 14 | 93 | 219.73 |
| | **RES 2** | 338 | 280.54 | 83 | 23 | 17 | 90 | 140.07 |
| | **RES 3** | 81 | 60.75 | 75 | 21 | 25 | 22 | 85.70 |
| **AVERAGE** | | | | | | | | |
| | **RES 1** | 471.63 | 399.41 | 84.75 | 23.25 | 15.25 | 94.75 | 152.51 |
| | **RES 2** | 381.25 | 300.71 | 79.00 | 23.25 | 21.00 | 93.00 | 150.69 |
| | **RES 3** | 92.25 | 63.30 | 69.25 | 19.50 | 30.75 | 57.75 | 59.68 |

**Petrophysical Characteristics of Reservoir 1**

Based on table 3, RES1 across all the wells, has gross and net thickness ranging from 392ft to 508.5ft and 337.12ft to 441.09ft with an average 471.63ft and 399.41ft respectively. Net-to-Gross ranges from 82% to 87% with an average of 84.75%. Effective Porosity ranges from 22% to 25% with an average of 23.25%. Volume of shale ranges from 13% to 18% with an average of 15.25%. Water saturation and permeability range from 88% to 100% and 140.07mD to 219.73mD respectively with an average of 82.50% and 152.51mD. Based on porosity and permeability, the reservoir quality is good and has good fluid storage and flow capacity.

**Petrophysical Characteristics of Reservoir 2**

This reservoir (RES 2) has gross and net thickness ranging from 338ft to 410ft and 280.54ft to 328ft respectively with an average of 381.25ft and 300.71ft respectively. Net-to-Gross ranges from 76% to 83% with an average of 79%. Effective Porosity ranges from 22% to 24% with an average of 23.25%. Volume of shale ranges from 17% to 24% with an average of 21%. Water saturation and permeability range from 83% to 100% and 110.18mD to 176.26mD respectively with an average of 93.00% and 150.69mD. Based on porosity and permeability, the reservoir quality is good and has the capacity for both storage and transmissivity.

**4.4. Petrophysical Characteristics of Reservoir 3**

From this study, RES 3 has gross and net thickness ranging from 62ft to 121ft and 42.16ft to 77.7ft respectively with an average of 92.25 and 63.3ft respectively. Net-to-Gross ranges from 74% to 68% with an average of 79%. Effective Porosity ranges from 18% to 21% with an average of 19.50%. Volume of shale ranges from 25% to 40% with an average of 30.75%. Water saturation and permeability range from 22% to 98% and 37.28mD to 85.70mD respectively with an average of 57.75% and 59.68mD. Based on porosity and permeability, the reservoir quality is fair and has moderate storage and fair deliverability in that if it is exploited, it may require stimulation.

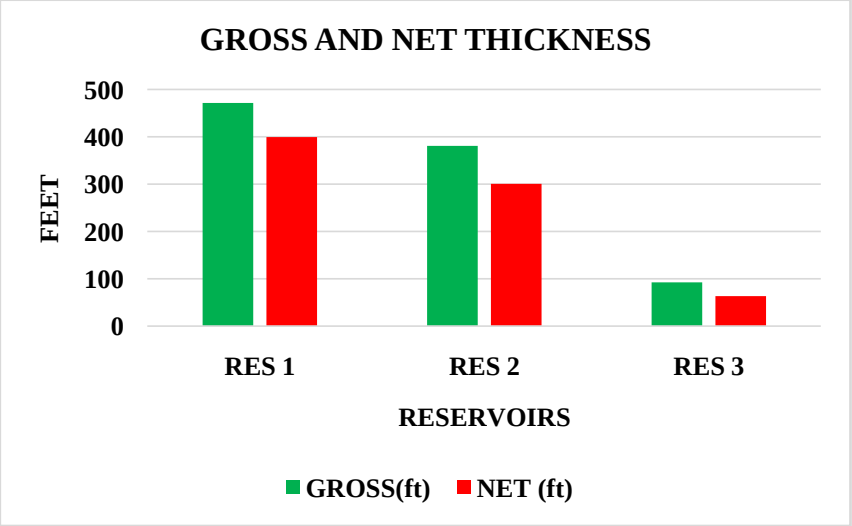


Figure 5: Histogram plot of average reservoir Gross and Net thickness

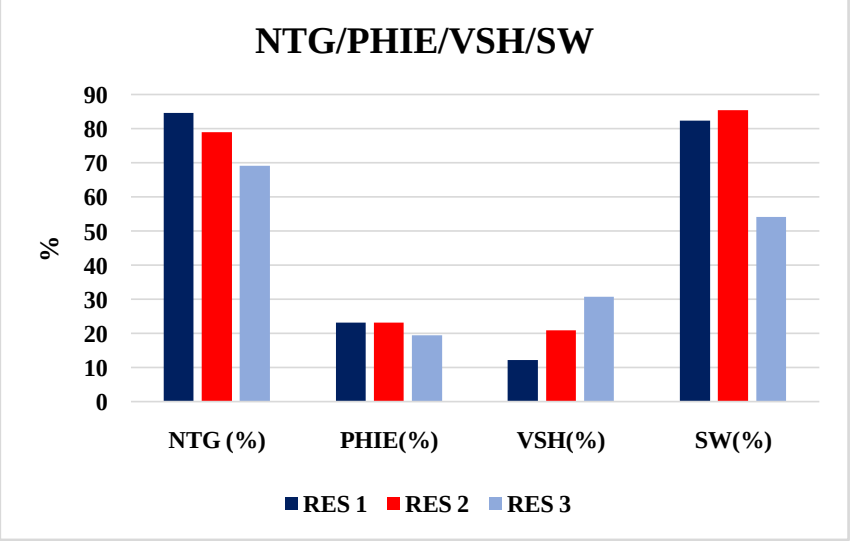


Figure 6: Histogram plot of average reservoir Net-to-Gross, Effective porosity, Volume of Shale and Water saturation

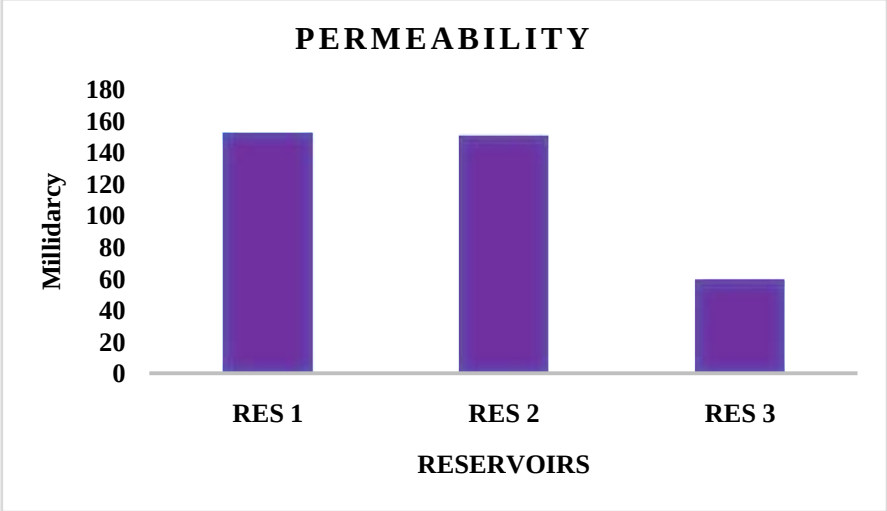


Figure 7: Histogram plot of average reservoir Permeability

**Comparative Analysis**

Utilizing figure 7, the gross and net thickness of reservoir RES1 and RES 2 are most promising compared to the deeper reservoir (Res 3). Figure 4.4 also show that RES 1 and RES 2 have good NTG compared to RES 3, based on RES 1 and RES 2 also have exhibit good porosity compared to RES 3, RES3 has the least VSH followed by RES 2 and RES 3 with the highest VSH and RES 1 and 2 have the highest water saturation compared to RES 3. The water saturation is not well specific but the average of both saturated and under saturated reservoirs. To this end some wells might have higher hydrocarbon saturation inferably lower water saturation compared to others. Finally, RES 1 and 2 have better permeability values compared to RES 3.

**RESERVOIR MAPPING**

To map the hydrocarbon bearing reservoirs (RES 1, RES 2 and RES 3) delineated via well log on seismic, the wells were integrated into seismic using the available checkshot data. In this case, a resultant synthetic seismogram was generated in other to ensure the reservoir tops are tied to their true corresponding reflections (Figure 4.6)

Within the time window of about 2200ms to 3000ms, the three reservoirs were mapped as illustrated in figure 4.7. All the three reservoirs were developed into a prospect because they all have a 3-way fault closure. From the hydrocarbon typing logs (Density and Neutron porosity), RES 1, 2 and 3 were most likely gas/ oil, gas and oil respectively. However, RES 1 most likely had Gas-Oil Contact (GOC) at -9496ftss and Oil Water Contact (OWC) at -9533ftss with a predicted gas pay thickness (PGT) of 22.15ft (6.75m) and Oil pay thickness (OPT) of 37ft (11.28m). RES 2 most likely had Gas-Water contact (GWC) at -10523ftss with a predicted gas pay thickness of 28ft (8.5m). RES 3 most likely had Oil-water contact at -11200ftss with predicted oil pay thickness of about 92.53ft (28.30m). The interpreted seismic section reveals a moderately dipping stratigraphic succession characterized by laterally continuous reflections across the line. A major listric fault forms the dominant structural elements, producing clear reflector offsets and establishing fault-bounded compartments. Thickness variations adjacent to the fault indicate syn-depositional activity that influenced sediment distribution. Reservoir horizons tied to the wells show strong, continuous seismic signatures, enabling reliable correlation across the section (Fig. 4.8). The downthrown block exhibits slightly thicker intervals, suggesting localized depocentres with potentially enhanced reservoir development. The structural map confirms a well-defined closure associated with updip portion of the line, where wells are positioned.

Table 4: Contact information and Predicted gas and oil pay thickness

| Reservoir | GOC (ftss) | OWC (ftss) | GWC (ftss) | PGT (ft) | OPT (ft) |
|---|---|---|---|---|---|
| **RES 1** | 9496 | 9533 | - | 22.15 | 37 |
| **RES 2** | - | - | 10523 | 28 | - |
| **RES 3** | - | 11200 | - | - | 28.30 |

Furthermore, after mapping the reservoirs across the seismic, reservoir representative time maps Fig. 4.6 were generated for further studies

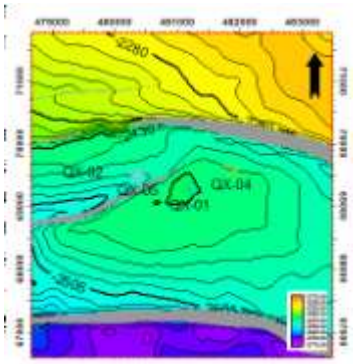


Figure 8: Synthetic seismogram along QX-5

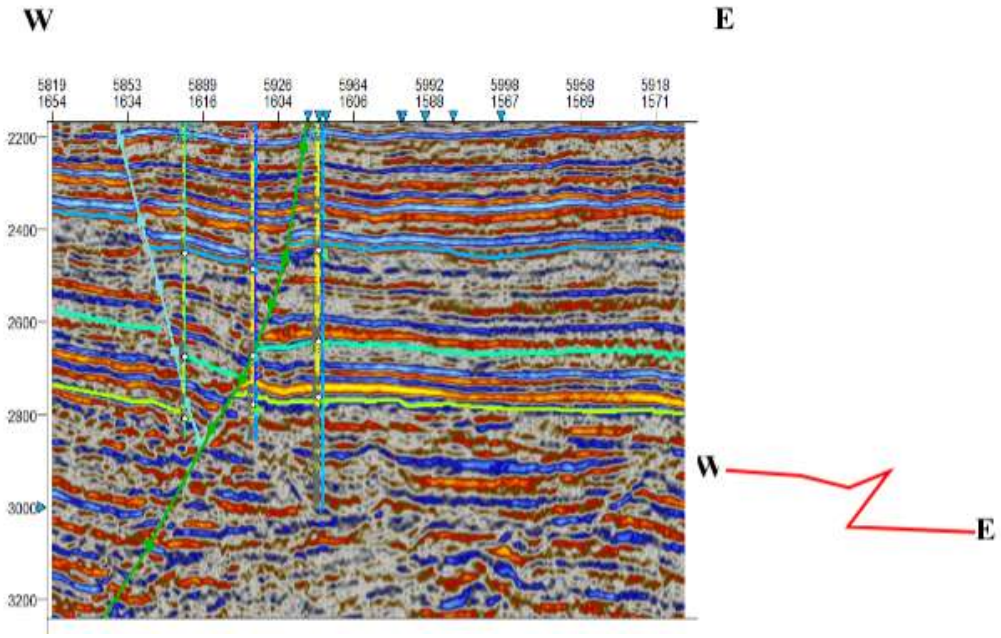


Figure 9: Arbitrary Seismic section along all the wells showing all the Reservoirs mapped

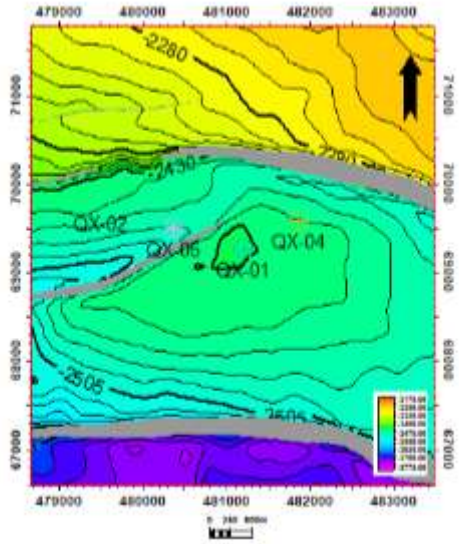


Figure 10: Time structural Map for RES 1

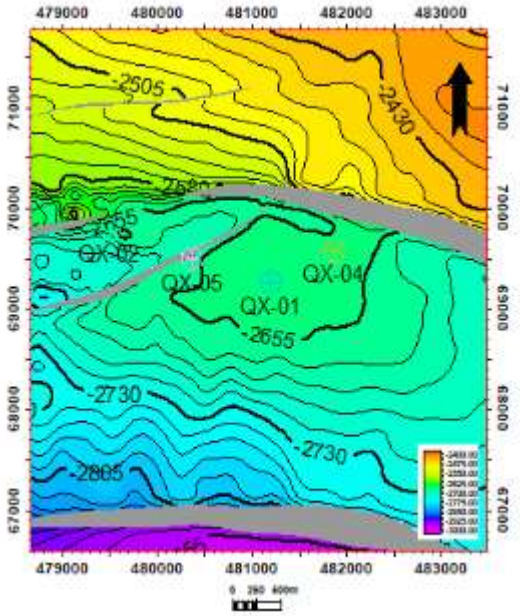


Figure 11: Time structural Map for RES2

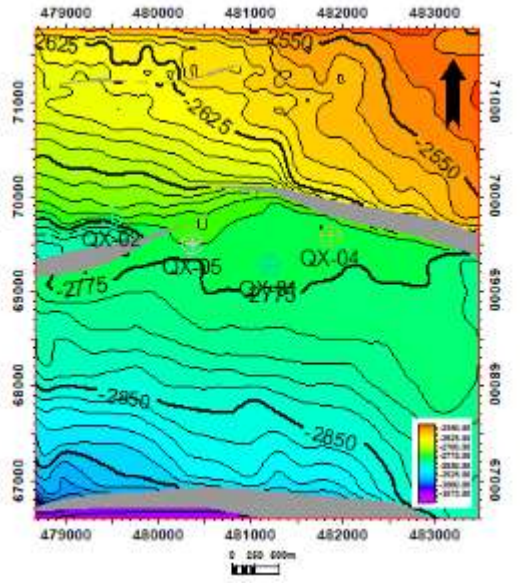


Figure 12: Time structural Map for RES3

**RESERVOIR GEOPHYSICS**

Root Mean Square (RMS) amplitude was utilized to ascertain pore filled and fluid contact most of. The result from the attribute analysis was used to calibrate petrophysical log evaluation especially porosity to check for consistency. The windows used for this extraction was restricted to the time window that corresponds to the reservoir's gross thickness. Hence, the RMS amplitude extraction was carried out for all the reservoirs based on the polarity type at the top of the reservoir. On this note, RES1, RES 2 and RES 3 utilized peak, trough and zero crossing -/+ polarities respectively.

Based on the amplitude map in figure 10-12, Res 1 is characterized by clearly defined amplitude shutoff across the hydrocarbon water interface as amplitude conforms excellently to structure. It also further affirms the likelihood of the good porosity and permeability gotten from the petrophysical evaluation. RES 2 on the other hand showed a dull and patchy amplitude with no clear amplitude shutoff to define hydrocarbon water contact. In this situation amplitude was slightly not consistent with the petrophysical result but it would be reliable most likely. Based on the amplitude map also, RES 3 showed conformance to structure and a strong hydrocarbon-brine shutoff notwithstanding the fair petrophysical result from well location other reservoir

location showed good reservoir quality based on the amplitude map although amplitude observably dull in some part.

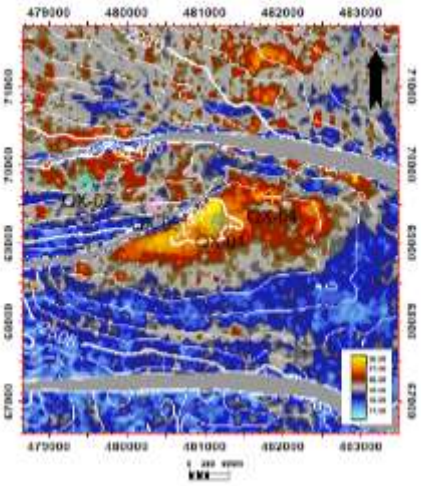


Figure 13: RMS amplitude maps for RES 1.

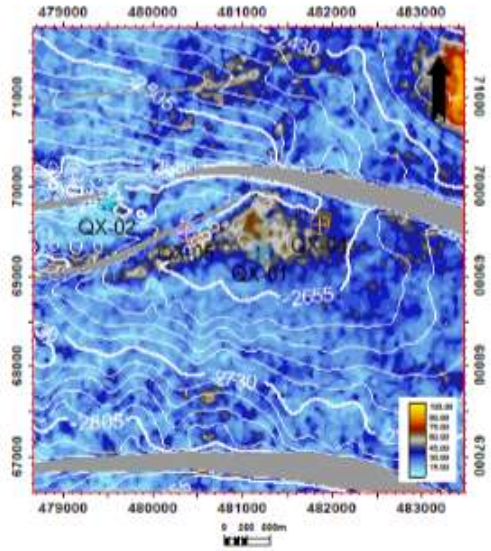


Figure 14: RMS amplitude maps for RES 2.

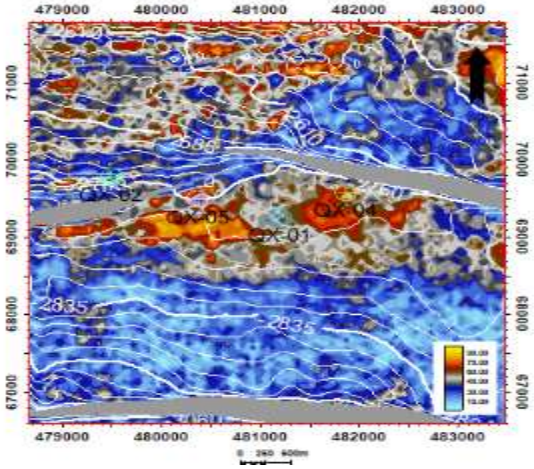


Figure 15: RMS amplitude maps for RES 3.

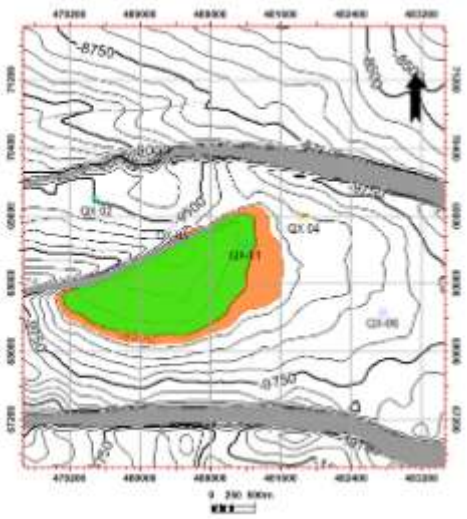


Figure 16: Depth structural maps for RES 1.

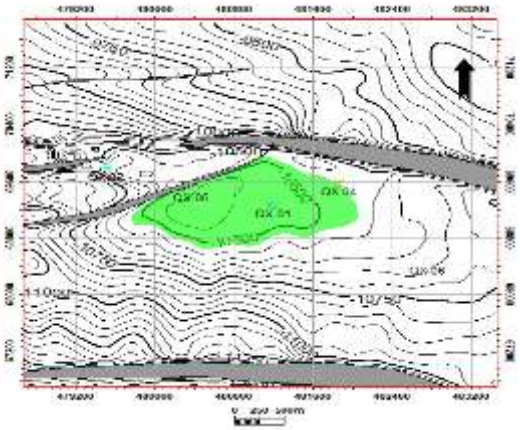


Figure 17: Depth structural maps for RES 2.

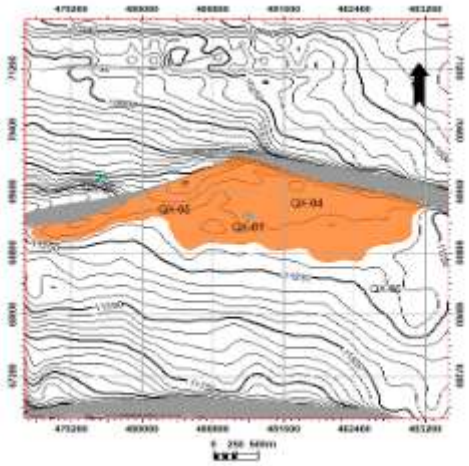


Figure 18: Depth structural maps for RES 3.

**VOLUMETRIC ESTIMATION**

Time map structural map was converted into depth structural map using a simple velocity model as stated in the methodology. Hydrocarbon high case contact information was displayed on the depth map is shown

in figure 21. Based on this, reservoir area was deciphered and calculated. For RES 1, oil and gas area was estimated to be 427.33 acre and 601.23 acre respectively. For Res 2, the area covered by gas was also estimated to 459.04 acre. For RES 3, Oil area was estimated to be 776.391 acre.

Based on the above and coupled with the result of the petrophysical evaluation, the Stock Tank Oil Initially in Place (STOIIP) and Gas Initially in Place (GIIP) volumes were estimated for the representative reservoirs as shown in Table 4.4. Also, Monte Carlo uncertainty estimation was carried out to determine High case scenario (P10), Mid case scenario (P50) and Base case scenario (P90). Outstanding observation from the estimation was that STOIIP of RES 1 seems to be lower than RES 3 basically because of its high-water saturation and lower oil pay thickness.

In sum, the total QX field most likely (P50) Oil volume is 64.40 MMSTB while most likely gas volume is 12.20 BCF.

Table 5: Result of the Volume Estimation

| **Reservoir** | **STOIIP (MMSTB)** | | | **GIIP (BCF)** | | |
|---|---|---|---|---|---|---|
| **CASES** | **P10** | **P50** | **P90** | **P10** | **P50** | **P90** |
| **RES 1(MC)** | 9.20 | 6.13 | 3.07 | 4.68 | **2.66** | **1.33** |
| **RES 2(MC)** | - | - | - | 14.31 | 9.54 | 4.77 |
| **RES 3(MC)** | 87.41 | 58.27 | 29.14 | - | - | - |
| **TOTAL(Probabilistic)** | **93.90** | **64.40** | **35.10** | **17.26** | **12.20** | **7.14** |

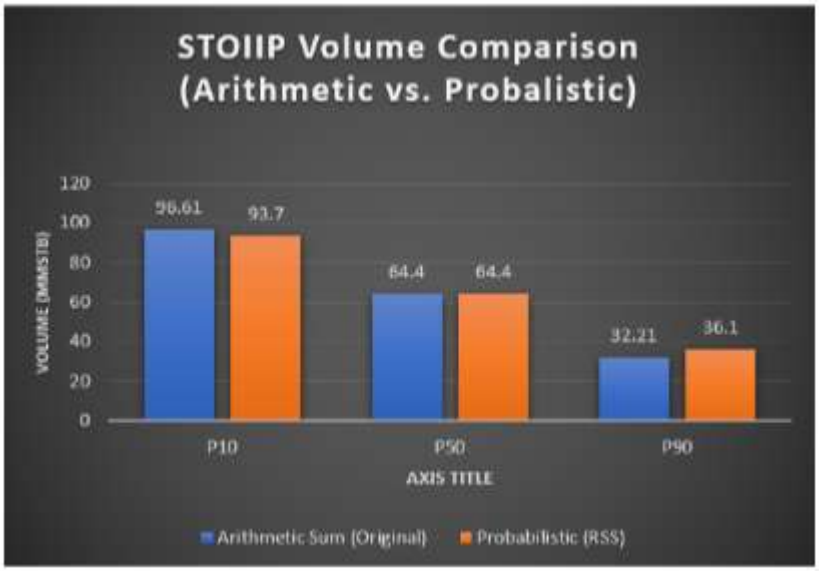


Figure 19: STOIIP Total Volume Comparsion

The final step in the volumetric assessment was the aggregation of the individual reservoir results to obtain the Total Field Volume. As shown in Figure (20), this step highlights the need for a probabilistic approach.The comparison between the initial Arithmetic Sum (the simple addition of P10, P50, and P90 values) and the Probabilistic Total (calculated using the Variance Addition Method, or RSS) confirms the principle of Portfolio Effect in reserves estimation.

i. P50 (Best Estimate): The P50 remains unchanged (64.40 MMSTB) because the mean (median) of independent distributions always adds arithmetically.

ii. P90 and P10 (Uncertainty Range): The arithmetic sum resulted in an artificially wide range (96.61 MMSTB P10 to 32.21 MMSTB P90). This range implies an unrealistically high probability of simultaneous extreme outcomes (all reservoirs being P10 or all being P90).

The Correction: The Probabilistic Total range (93.70 MMSTB P10 to 35.10 MMSTB P90) is narrower. This accurately reflects that when combining independent reservoirs, the high outcomes in one area are offset by the low outcomes in another, leading to a reduction in the overall uncertainty.

The final accepted volumetric estimates for the field are the Probabilistic Totals because they represent a statistically sound aggregation of the individual Monte Carlo simulation outputs.

i. The P90 volume (35.10 MMSTB) is the conservative, proved reserve estimate, indicating a 90% chance that the field contains at least this volume.
ii. The P10 volume (93.70 MMSTB) is the optimistic, possible reserve estimate, indicating only a 10% chance that the field volume will exceed this number.

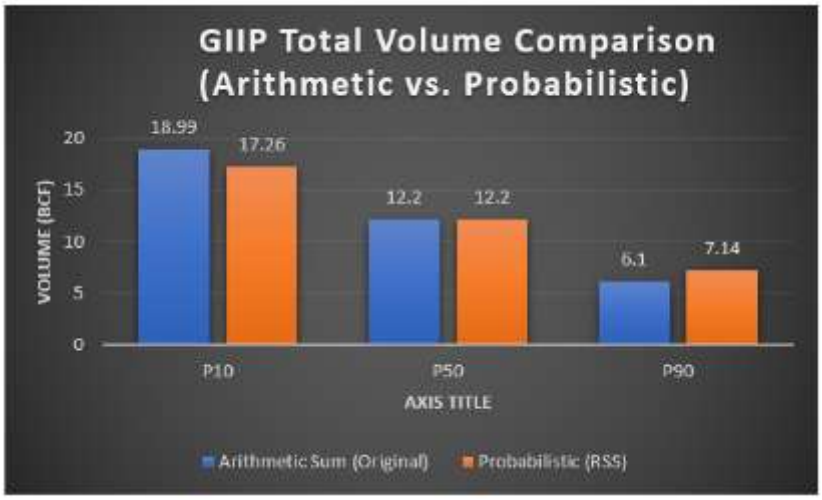


Figure 20: GIIP Total Comparsion

Probabilistic Aggregation of Gas Initially In Place (GIIP)

The same method as the STOIIP was used in the GIIP. This ensures consistency and statistical thoroughly across all estimated hydrocarbon volumes.

As shown in Figure (20) the analysis revealed a significant discrepancy between the initial arithmetic sum and the corrected probabilistic sum. The original arithmetic addition of the individual reservoir P10s and P90s yielded an artificially wide uncertainty range (P10: 18.99 BCF; P90: 6.10 BCF). This overstates the overall risk and opportunity by assuming all reservoirs would hit their extreme high or low estimates simultaneously . By applying the Variance Addition Method (RSS), the total GIIP volume was correctly determined to have a narrower range (P10: 17.26 BCF; P90: 7.14 BCF).

The necessity of the RSS method for GIIP aggregation reinforces the concept of the Portfolio Effect. Since the gas volumes in Reservoir 1 and Reservoir 2 are assumed to be statistically independent, combining them results in a lower overall risk.

i. The P90 conservative estimate increased from 6.10 BCF to 7.14 BCF, providing higher confidence in the minimum available gas reserves.
ii. The P10 optimistic estimate decreased from 18.99 BCF to 17.26 BCF, indicating that the extremely high volume is less likely to be achieved when the individual reservoir uncertainties are combined.

This analysis confirms that the final, accepted Total GIIP volume must be the Probabilistic Total (17.26 BCF / 12.20 BCF / 7.14 BCF) to accurately represent the uncertainty profile of the combined gas resource.

## VII. Conclusion

This study has provided an integrated qualitative and quantitative evaluation of the depositional environment and hydrocarbon potential of the QX Field in the Southeastern Niger Delta. The study applied well log interpretation, seismic attribute analysis, and volumetric modelling to assess three reservoir units (RES 1, RES 2, and RES 3), each deposited in different sedimentary settings ranging from channelized to lower shoreface environments. These depositional settings applied a control on the spatial distribution, geometry, and

petrophysical quality of the reservoirs, which is consistent with the geological of deltaic systems in the Niger Delta.

Petrophysical analysis showed that the reservoirs possess favourable reservoir characteristics, with net-to-gross ratios ranging from 69.25% to 84.75%, effective porosity between 19.5% and 23.25%, and moderate permeability values from 59.68 mD to 152.51 mD, indicating moderate-to-good quality reservoir rocks. Water saturation ranged from 57.75% to 94.75%, with corresponding hydrocarbon saturations indicating that the sands are capable of economically storing hydrocarbons. The volumetric estimates confirmed the presence of commercial hydrocarbon volumes, with a cumulative optimistic estimate of 64.40 MMSTB of oil and 12.20 BCF of gas, reinforcing the field's prospectivity.

The resultshows that combining petrophysical data, facies interpretation, and seismic attributes provides an effective approach to define reservoir zones and assess performance in the structurally complex QX Field. Three-way fault closures act as the main structural traps, confirming the importance of faulting in controlling hydrocarbon accumulation.

## References


[1]. Archie, G. E. (1942). The Electrical Resistivity Log as an Aid in determining Some Reservoir Characteristics. Petroleum Transactions of the American Institute of Mining, Metallurgical and Petroleum Engineering (AIME), 146, 54–62.

[2]. Archie, G. E. (1952). Classification of carbonate reservoir rocks and petrophysical considerations. AAPG Bulletin, 36(2), 278–298.

[3]. Asquith, G., & Krygowski, D. (2004). Basic Well Log Analysis (2nd ed.). AAPG.

[4]. Burke, K. (1972). Longshore drift, submarine canyons, and canyons on the Niger Delta. Journal of Geology, 80(5), 539-550.

[5]. Burke, K., Dessauvagie, T. F. J., & Whiteman, A. J. (1971). Opening of the Gulf of Guinea and geological history of the Benue Depression and Niger Delta. Nature Physical Science, 233(39), 51-55

[6]. Chopra, S., & Marfurt, K. J. (2007). Seismic Attributes for Prospect Identification and Reservoir Characterization. Society of Exploration Geophysicists (SEG) Publications.

[7]. Daukoru, C. M. (1994). Northern Delta Depobelt Portion of the Akata-Agbada Petroleum system, Niger Delta, Nigeria. Petroleum Association System, AAPG memoir 60. American Association of Petroleum Geologists (AAPG), Tulsa, 598–616.

[8]. Dake, L. P. (1978). Fundamentals of Reservoir Engineering. Elsevier.

[9]. Doust, H. (1990). Petroleum geology of the Niger Delta. Geological Society, London, Special Publications, 50, 365.

[10]. Doust, H., & Omatsola, E. (1989). Niger delta. In J. D. Edwards & P. A. Santogrossi (Eds.), Divergent/passive margin basins 48: Tulsa memoir Ok. American Association of Petroleum Geologists, pp. 201–238.

[11]. Doust, H., & Omatsola, E. (1990). Niger Delta. In J. D. Edwards & P. A. Santogrossi (Eds.), Divergent/Passive Margin Basins: AAPG Memoir 48. American Association of Petroleum Geologists, Tulsa, 48, 239–248.

[12]. Downey, J. D. (2005). Seismic sequence stratigraphy: Recent advances and applications. In J. R. Boles & T. M. Bown (Eds.), Geological Society of America Special Paper 392: Applied Stratigraphy: From Pre-Feldspar to Hydrocarbon Exploration (pp. 1–20). Geological Society of America.

[13]. Evamy, B. D., Haremboure, J., Kamerling, P., Knaap, W. A., Molloy, F. A., & Rowlands, P. H. (1978). Hydrocarbon habitat of Tertiary Niger delta. AAPG Bulletin, 62(1), 1–39.

[14]. Klett, T. R., Ahlbrandt, T. S., Schmoker, J. W., & Dolton, J. L. (1997). Ranking of the world's oil and gas provinces by known petroleum volumes. U.S. Geological Survey Open-file Report, p. 97-463 CD-ROM.

[15]. Kulke, H. (1995). In H. Kulke (Ed.), Regional Petroleum Geology of the World. Part II: Africa, America, Australia and Antarctica. Gebrüder Borntraeger, pp. 143–172.

[16]. Olowokere, M. T., Olobaniyi, S. B., & Aizebeokhai, A. P. (2019). Petrophysical Analysis of Hydrocarbon Reservoirs in the Western Niger Delta. Nigerian Journal of Geosciences, 55(2), 101–112.

[17]. Olowokere, S. A., Olayanju, G. M., & Omoshuyi, B. A. (2019). Petrophysical Evaluation of Hydrocarbon Potential in 'Z' Field, Western Niger Delta, Nigeria. Journal of Geoscience and Environment Protection, 7(9), 1–16.

[18]. Olowokere, M. T., Hassane, A., Alonge, M. A., & Ajibade, E. A. (2019). Hydrocarbon prospectivity determination of "eagle field", coastal swamp ii Niger delta. International Journal of Advanced Geosciences, 7(1), 52-57.

[19]. Olowokere, M. T., & Ojo, J. S. (2010). Fluid Detections and Lithology Discrimination using Lame Petrophysical Parameters from Simultaneous Inversion – using Northern North Sea, Norway. National Association of Petroleum Explorationists (NAPE) Int'l Bulletin, 22(1), 36–42.

[20]. Rider, M. (2002). The Geological Interpretation of Well Logs (2nd ed.). Whittles Publishing.

[21]. Rider, M. H., & Kennedy, M. (2011). The Geological Interpretation of Well Logs (3rd ed.). Rider-French.

[22]. Russell, B. H., Hedlin, K., Hitterman, F. J., & Lines, L. R. (2003). Fluid property discrimination with AVO, A Biot- Grassmann perspective. Geophysics, 68, 29–39.

[23]. Selley, R. C. (1985). Elements of petroleum geology. W. H. Freeman and Company, New York, 448pp.

[24]. Selley, R. C. (1998). Elements of petroleum geology. Department of Geology, Imperial College, London United Kingdom, 37–145.

[25]. Short, K. C., & Stauble, A. J. (1967). Outline of Geology of Niger Delta. American Association of Petroleum Geologists, Bulletin, 51, 761–779..

[26]. Slatt, R. M. (2006). Stratigraphic Reservoir Characterization for Petroleum Geologists, Geophysicists, and Engineers. Elsevier.

[27]. Society of Petroleum Engineers (SPE). (2018). Petroleum Resources Management System (PRMS). SPE, World Petroleum Council, American Association of Petroleum Geologists, Society of Petroleum Evaluation Engineers, Society of Exploration Geophysicists, Society of Petrophysicists and Well Log Analysts, and Latin American and Caribbean Petroleum Engineering Confederation.

[28]. Stacher, P. (1995). Present understanding of the Niger delta hydrocarbon habitat. In M. N. Oti & G. Postma (Eds.), Geology of Deltas. A. A. Balkema, Rotterdam, pp. 257–267.

[29]. Taylor, J. R. (1997). An Introduction to Error Analysis: The Study of Uncertainties in Physical Measurements (2nd ed.). University Science Books.

[30]. Tuttle, M. L. W., Charpentier, R. R., & Brownfield, M. E. (1990). Tertiary Niger Delta (Akata-Agbada) Petroleum System (No. 701901), Niger Delta Province, Nigeria, Cameroon, and Equatorial Guinea, Africa. In USGS (Ed.), The Niger Delta Petroleum

System: Niger Delta Province, Nigeria, Cameroon, and Equatorial Guinea, Africa. U.S. Department Of The Interioru.S. Geological Survey, Denver, Colorado.

[31]. Tuttle, M. L., Charpentier, R. R., & Brownfield, M. E. (1999). The Niger delta Petroleum System: Niger delta Province, Nigeria, Cameroon, and Equatorial Guinea, Africa (pp. 99–50). US Department of the Interior, US Geological Survey.

[32]. Vail, P. R., Mitchum, R. M., Jr., Todd, R. G., Widmier, J. M., Thompson, S., III, Sangree, J. B., Bubb, J. N., & Hatlelid, W. G. (1977). Seismic stratigraphy and global changes of sea level. In C. E. Payton (Ed.), Seismic Stratigraphy—Applications to Hydrocarbon Exploration (Vol. 26, pp. 49–212). American Association of Petroleum Geologists (AAPG) Memoir.

[33]. Walker, R. G. (1978). Deep-water sandstone facies and ancient submarine fans: models for exploration for stratigraphic traps. AAPG Bulletin, 62(6), 932–966.

[34]. Walker, R. G., & James, N. P. (Eds.). (1992). Facies Models: Response to Sea Level Change. Geological Association of Canada, GeoText 1.

[35]. Weber, K. J. (1971). Sedimentological aspects of oil fields in the Niger Delta. Geologie en mijnbouw, 50, 559–576.

[36]. Weber, K. J. (1987). Hydrocarbon distribution patterns in Nigerian growth fault structures controlled by structural style and stratigraphy. Journal of Petroleum Science and Engineering, 1, 91–104.

[37]. Weber, K. J. (1986). Hydrocarbon distribution patterns in Nigerian growth fault structures controlled by structural style and stratigraphy. American Association of Petroleum Geologists (AAPG) Bulletin, 70, 661–662.

[38]. Weber, K. J., & Daukoru, E. M. (1975). Petroleum geology of the Niger Delta. Proceedings of the Ninth World Petroleum Congress, 2, Geology: Applied Science Publishers, Ltd., London, pp. 210–221.

[39]. Weber, K. J., & Daukoru, E. M. (1975). Petroleum geology of the Niger delta. Earth Science Journal, 2(1), 210–221.

[40]. Weber, K. J., & Daukoru, E. M. (1975). Petroleum geology of Niger Delta. 9th World Petroleum Congress, 2, 209–221.

[41]. Whiteman, A. J. (1982). Nigeria: It petroleum geology, resources and potential. London, Graham and Trothman, 1:166.

[42]. Whiteman, A. J. (2012). Nigeria: its petroleum geology, Resources and Potential Volume 1. Springer Science and Business Media.